

THE EFFECTS OF ZOLEDRONATE AND RALOXIFENE
COMBINATION THERAPY ON DISEASED MOUSE BONE

A Thesis

Submitted to the Faculty

of

Purdue University

by

Katherine M. Powell

In Partial Fulfillment of the

Requirements for the Degree

of

Master of Science in Biomedical Engineering

May 2019

Purdue University

Indianapolis, Indiana

THE PURDUE UNIVERSITY GRADUATE SCHOOL
STATEMENT OF THESIS APPROVAL

Dr. Joseph M. Wallace, Chair

Department of Biomedical Engineering

Dr. Matthew R. Allen

Department of Anatomy and Cell Biology

Dr. Hiroki Yokota

Department of Biomedical Engineering

Approved by:

Dr. Julie Ji

Head of the Graduate Program

TABLE OF CONTENTS

	Page
LIST OF TABLES	v
LIST OF FIGURES	vi
LIST OF SYMBOLS	vii
LIST OF ABBREVIATIONS	viii
ABSTRACT	ix
1 INTRODUCTION	1
1.1 Bone Overview	1
1.2 Poor Bone Quality	2
1.3 Bone Remodeling	3
1.4 Bisphosphonates	3
1.5 Raloxifene	4
1.6 Gap and Plan of Attack	5
2 MATERIALS AND METHODS	6
2.1 Animals and Treatment	6
2.2 Microcomputed Tomography (μ CT) and Architectural Analysis	6
2.3 Three-point Bending Mechanical Testing to Failure	7
2.4 Fracture Toughness Testing	7
2.5 Statistical Analysis	8
3 RESULTS	9
3.1 Trabecular Architecture and Mineralization	9
3.2 Cortical Geometry at the Femoral Mid-Diaphysis	9
3.3 Femoral Mechanical Strength and Stiffness	13
3.4 The Effect of Combination Treatment on Fracture Toughness	19
4 CONCLUSION	21

	Page
4.1 Discussion	21
4.2 Limitations and Future Work	24
LIST OF REFERENCES	26

LIST OF TABLES

Table	Page
3.1 WT Cortical Geometry	11
3.2 OIM+/- Cortical Geometry	12
3.3 WT Structural Mechanical Properties	15
3.4 OIM+/- Structural Mechanical Properties	16
3.5 WT Tissue-Level Mechanical Properties	17
3.6 OIM+/- Tissue-Level Mechanical Properties	18

LIST OF FIGURES

Figure	Page
3.1 Treatment Effects on Trabecular Properties.	10
3.2 Treatment Effects on Mechanical Properties.	14
3.3 Effects of Treatment on Fracture Toughness.	20

LIST OF SYMBOLS

- * Indicates significant change from control within each genotype at $p \leq 0.05$

LIST OF ABBREVIATIONS

BMD	Bone Mineral Density
BP	Bisphosphonate
BV/TV	Bone Volume Fraction
CSA	Cross Sectional Area
Displ.	Displacement
I_{max}	Maximum Moment of Inertia
I_{min}	Minimum Moment of Inertia
OIM+/-	Heterozygous
Pm.	Perimeter
RAL	Raloxifene
Th.	Thickness
TMD	Tissue Mineral Density
WT	Wildtype
ZOL	Zoledronate

ABSTRACT

Powell, Katherine M. M.S.B.M.E., Purdue University, May 2019. The Effects of Zoledronate and Raloxifene Combination Therapy on Diseased Mouse Bone. Major Professor: Joseph M. Wallace.

Current interventions used to reduce skeletal fragility are insufficient at enhancing bone across multiple hierarchical levels. Bisphosphonates, such as Zoledronate (ZOL), treat a variety of bone disorders by increasing bone mass and bone mineral density to decrease fracture risk. Despite the mass-based improvements, bisphosphonate use has been shown to compromise bone quality. Alternatively, Raloxifene (RAL) has recently been demonstrated to improve tissue quality and overall mechanical properties by binding to collagen and increasing tissue hydration in a cell-independent manner. We hypothesized that a combination of RAL and ZOL would improve mechanical and material properties of bone more than either monotherapy alone by enhancing both quantity and quality of bone. In this study, wildtype (WT) and heterozygous (OIM+/-) male mice from the Osteogenesis Imperfecta (OI) murine model were treated with either RAL, ZOL, or RAL and ZOL from 8 weeks to 16 weeks of age. Combination treatment resulted in higher trabecular architecture, cortical mechanical properties, and cortical fracture toughness in diseased mouse bone. Two fracture toughness properties, direct measures of the tissues ability to resist the initiation and propagation of a crack, were significantly improved with combination treatment in OIM+/- compared to control. There was no significant effect on fracture toughness with either monotherapy alone in either genotype. Following the mass-based effects of ZOL, bone volume fraction was significantly higher with combination treatment in both genotypes. Similar results were seen in trabecular number. Combination treatment resulted in higher ultimate stress in both genotypes, with RAL additionally in-

creasing ultimate stress in OIM+/- . RAL and combination treatment in OIM+/- also produced a higher resilience compared to the control. Given no significant changes in cortical geometry, these mechanical alterations were likely driven by the quality-based effects of RAL. In conclusion, this study demonstrates the beneficial effects of using combination therapy to increase bone mass while simultaneously improving tissue quality, especially to enhance the mechanical integrity of diseased bone. Combination therapies could be a future mechanism to improve bone health and combat skeletal fragility on multiple hierarchal levels.

CHAPTER 1. INTRODUCTION

1.1 Bone Overview

Bone is organized in a hierarchal multiscale fashion with each level contributing to its mechanical integrity. At the nanostuctural level, bone is a composite matrix consisting of mineral, collagen, and noncollagenous proteins. The composite surrounds and supports three types of bone cells: osteoblasts, osteoclasts, and osteocytes. These cells produce and maintain the structure of the bone. The cells come together to form lamellae, which layer upon each other to create macroscopic cortical and trabecular bone. [1]

While it is often thought that bone mass and size affect the majority of the bones mechanical behavior, the intrinsic quality of bone tissue can dramatically influence the mechanical integrity of the bone. Tissue quality refers to the bones chemical and physical properties without regard to its mass or macroscopic structure. This includes the bones inherent ability to resist load. Some measurable parameters of bone quality include tissue mineral density, chemical composition, degree of enzymatic collagen cross-linking, microdamage, and accumulation of advanced glycation end-products (AGEs). These parameters affect the microscopic composite and can alter the bones ability to absorb energy and resist fracture. [2–6]

Numerous bone diseases and disorders cause skeletal fragility and increased fracture risk. The American public faces 1.5 million fractures each year resulting in an expense of over \$18 billion just for direct care. [7] Current diagnosis tools and treatment for skeletal fragility focus on improving bone mass and bone mineral density (BMD). Unfortunately, the effect of bone tissue quality at the microscopic level is

overlooked and is not targeted for therapy. Increasing bone mass, while simultaneously improving the quality of collagen-mineral tissue composite, has the potential to become a unique strategy that improves fracture resistance and optimally reduces skeletal fragility.

1.2 Poor Bone Quality

Numerous diseased states can cause bone quality to be compromised. Tissue at the microscopic level can be altered, leading to increased fracture risk and poor bone health. For example, diabetes can produce negative consequences and cause increased fractures compared to normal healthy bone. In diabetic patients, it has been shown that their increase blood glucose levels can cause an accumulations of AGEs in the collagen mineral matrix. Though these patients normally have an average BMD, diabetics have increased fracture risk due to their poor bone quality. [8]

Alterations in tissue quality can also be genetic. Osteogenesis imperfecta (OI) is a genetic disease in bone caused by a mutation in Type I collagen or related proteins. Over 1500 independent genome alterations have been identified that lead to mutated OI collagen. This wide variety of mutations leads to varying clinically severity of the disease. Patients with a mild form of OI may only experience a few fractures throughout their lifetime, but those with a severe form may experience innumerable breaks, often resulting from low energy impact. [9,10]

OI is deemed brittle bone disease due to its dominant phenotype of increased fracture risk. This risk of fractures roots from the poor quality bone tissue of OI. The mutated collagen leads to poor formation of the triple helical structure, driving quality-based deficiencies in the collagen-mineral composite. [11–13] These microscopic changes induce macroscopic effects and cause brittle bones and frequent fractures in patients suffering from the disease.

Current treatments used to combat OI and other modes of skeletal fragility do not target the quality of the bone. Investigating therapeutics that beneficially alter the

collagen mineral composite, rather than just increasing bone mass, offers a unique strategy to combat fragility and increase the bones ability to resist fracture.

1.3 Bone Remodeling

Remodeling is the process of bone formation and resorption that the skeleton undergoes to keep bones at optimal health. Remodeling removes areas of old or damaged tissue, non-viable cells, or tissue with suboptimal properties, and replaces these regions with new cells and tissue. Osteoclasts resorb and degrade bone, while osteoblasts are the cells that form new bone. [14,15]

Osteocytes differentiate from osteoblasts that became trapped in the bone matrix during formation. Osteocytes encompass over 90% of the cells in the matrix and reside as chemical and mechanical sensor cells. Increasing evidence suggests that osteocytes help regulate osteoblast and osteoclasts through mechanical and hormonal cues. For example, osteocytes can detect microdamage in the matrix and signal to the osteoclasts that the region needs to be remodeled. [16]

Diseases and disorders can occur when the remodeling process is disrupted. For example, age-related osteoporosis presents due to a remodeling imbalance and causes bone loss and fragility. In this case, age-related estrogen deficits lead to the prolonged lifespan of osteoclasts, which results in more bone resorption that is not balanced by formative refilling. [17] Over time, this results in loss of bone tissue and ultimately bone fragility.

1.4 Bisphosphonates

Bisphosphonates (BPs) have been the gold standard treatment for numerous bone disorders for the past 30 years. BPs target osteoclasts and decrease their activity, which ultimately leads to the disruption of the bone remodeling process. BPs have a high affinity for bone mineral. When osteoclasts attach to the surface and try to resorb bone, the BPs act against them and decrease their activity.

The type of class determines the mechanism upon which BPs act. Non-nitrogen-containing BPs are taken up by osteoclasts upon resorption and disrupt their cellular function, ultimately inducing apoptosis and overall decrease of osteoclasts. Nitrogen-containing BPs stabilize the bone matrix and prevents it from being resorbed, reducing the efficacy of the osteoclasts. Zoledronate (ZOL) is an example of a nitrogen-containing BP and is considered one of the most potent BPs. [18]

BPs increase bone mineral density which leads to decreased fracture risk in diseases such as postmenopausal osteoporosis, Pagets disease, metastatic osteolytic lesions, and more recently, Osteogenesis Imperfecta. [19–21] Bisphosphonates target osteoclasts and decrease their activity, which ultimately leads to the disruption of the bone remodeling process. [22] Despite the increase in bone mass that occurs with the use of BPs, long term use may have unintended consequences.

Tissue quality at the microscopic level is compromised with bisphosphonate use. The disruption of bone remodeling shuts down the bone repair mechanism which can lead to the accrual of microdamage in the tissue, making the tissue more susceptible to failure. [23] There is also an increase in non-enzymatic cross linking in the collagen matrix that has been correlated with reduced post-yield mechanical properties and reduced bone toughness. [24–26] Although bisphosphonates have positive mass-based effects in bone, tissue quality may not be optimal, making these treatments insufficient to overcome mechanical deficits common with disease. There is a need to simultaneously improve tissue quality while increasing mass.

1.5 Raloxifene

Raloxifene (RAL) is in a different class of FDA-approved drugs used to treat osteoporosis in post-menopausal women. The drug primarily acts in a cell-dependent manner as a Selective Estrogen Receptor Modulator (SERM) and combats bone loss by binding and signaling through estrogen receptors on osteoblasts. [27] Clinically, RAL reduces fractures by 50% but with modest changes in remodeling and BMD.

[28–30] This observation suggests that the changes in mechanical integrity are driven by tissue quality changes versus altered mass or architecture.

Recent work has demonstrated that RAL also exhibits cell-independent behavior by binding to collagen and increasing tissue hydration, leading to enhanced mechanical properties and fracture resistance. [31,32] These cell-independent, material-based changes provide a unique opportunity to beneficially alter bone fracture resistance through changes in tissue quality, especially in disease states that are driven by inferior tissue properties.

1.6 Gap and Plan of Attack

Current treatments used to treat bone fragility are insufficient at improving bone across multiple hierarchical levels. The purpose of this study was to use a combination treatment to target different levels of bone to enhance overall mechanical integrity. It was hypothesized that using the mass-based effects of BPs, in conjunction with the tissue level improvements noted with RAL, the combinatorial treatment would improve bone mechanical properties and fracture resistance more than either monotherapy alone.

The Osteogenesis Imperfecta murine (oim) model of OI was used for this study. The oim model allows for investigation of how combination treatments impact the phenotype of a quality-based disease state [33], where adding more, poor quality, tissue with BPs might not be enough to overcome mechanical deficiencies.

CHAPTER 2. MATERIALS AND METHODS

2.1 Animals and Treatment

All protocols and procedures were performed with prior approval from the IU School of Medicine IACUC. Male wild-type (WT) and heterozygous (OIM +/-) mice were bred from heterozygous parental strains on a C57BL/6 background. Mice (n=13-15 per group) were injected with either RAL (0.5 mg/kg; 5x/week), zoledronate (ZOL; 80 $\mu\text{g}/\text{kg}$; at 8 weeks and 12 weeks of age), or the combination. Untreated controls were also included. These dosages were chosen based on previous research showing efficacy in vivo. [34–37] Treatments began at 8 weeks of age and extended for 8 weeks. At 16 weeks of age, the mice were euthanized, at which time right femora and tibiae were harvested, stripped of soft tissue, and frozen in saline-soaked gauze at -20°C .

2.2 Microcomputed Tomography (μCT) and Architectural Analysis

To determine the effects of treatment on bone architecture, right femora and right tibiae were scanned at 10-micron resolution (Skyscan 1172, Bruker). Scans were performed using a 0.7-degree angle increment, two frames averaged, through a 0.5mm Al filter ($V = 60\text{kV}$, $I = 167\mu\text{A}$). Images were reconstructed (nRecon) and calibrated to hydroxyapatite-mimicking phantoms (0.25 and $0.75\text{ g}/\text{cm}^3$ Ca-HA). 1-mm trabecular regions were selected and quantified using CT Analyzer (CTAn). The region for the femora was selected at the distal metaphysis and extended 1mm proximally from the most proximal portion of the growth plate. The trabecular region for the tibiae was selected at the proximal metaphysis and extended 1-mm distally

from the most distal portion of the growth plate. A 1-mm cortical region was selected at approximately 50% length of the femur, then analyzed with a custom MATLAB program to obtain architectural properties. [38]

2.3 Three-point Bending Mechanical Testing to Failure

Each femora was tested to failure in three-point bending (support span at 8mm) with the anterior surface in tension. The bones were loaded at a displacement control rate of 0.25 mm/sec while the sample remain hydrated with PBS. Cross sectional cortical properties at the femoral mid-point were obtained with μ CT images as described above. These properties were used to map load-displacement data into stress-strain data using standard engineering equations as previously reported. [39]

2.4 Fracture Toughness Testing

Fracture toughness of the right tibiae was measured using a linear elastic fracture mechanics approach. [40,41] A notch was made on the anteromedial side of the tibia, at approximately 50% length, using a scalpel blade lubricated with a 1 μ m diamond suspension. The tibiae were notched into the medullary cavity to a depth not exceeding the bones midpoint. They were then tested to failure in 3 point bending at a displacement control rate of 0.001 mm/sec with the notched surface in tension. The load point was positioned directly above the notch site.

After mechanical testing, the bones were cleansed of marrow and dehydrated using an ethanol gradient (70-100%) and a vacuum desiccator. Following sputter-coating with gold, the cross-sectional fracture surface was imaged with scanning electron microscopy (SEM). The angles of stable and unstable crack growth were obtained from the images and, along with geometric properties from μ CT data, a custom MATLAB program calculated stress intensity factors for crack initiation, maximum load, and fracture instability.

2.5 Statistical Analysis

Within each genotype, a One-Way ANOVA with post-hoc Dunnetts test was used to statistically analyze the effect of each treatment versus control. Analysis was performed using GraphPad Prism (v.8) with a significance level at 0.05.

CHAPTER 3. RESULTS

3.1 Trabecular Architecture and Mineralization

Bone volume fraction in the femoral distal metaphysis was significantly higher compared to control in both genotypes with ZOL monotherapy and combination treatment, but not with RAL monotherapy (Fig. 3.1). In both genotypes, trabecular number was significantly increased with ZOL alone and with combinatorial therapy, but not with RAL alone. Although trabecular thickness trended upward with RAL in both WT (+7.1%) and OIM+/- (+5.8%), it only reached significance with combination treatment which substantially increased in both genotypes (WT:+24.7%; OIM+/-:+20.9%). As a result, trabecular spacing was decreased in both genotypes with ZOL alone and combination therapy. Tissue mineral density (TMD) was significantly elevated with the combination treatment in both genotypes. RAL monotherapy significantly increased TMD in the WT mice and trended upward in OIM+/- . ZOL had no effect on TMD in either genotype. Identical results were demonstrated at the proximal tibial metaphysis (data not shown).

3.2 Cortical Geometry at the Femoral Mid-Diaphysis

There were no significant changes with either monotherapy or combinatorial treatment in any cortical properties at the femoral mid-diaphysis (Table 3.1, Table 3.2).

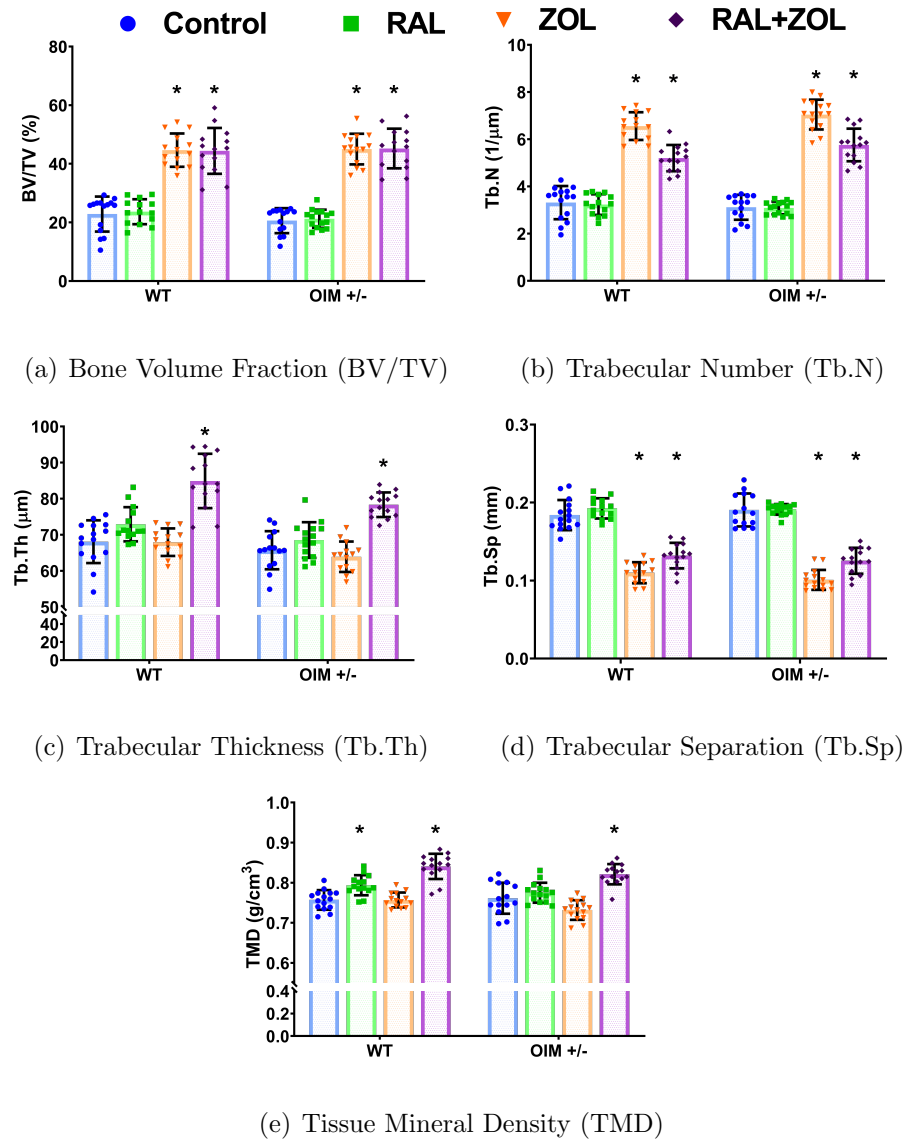


Fig. 3.1: Treatment Effects on Trabecular Properties.

Table 3.1: WT Cortical Geometry

Property	Control	RAL	ZOL	RAL+ZOL
Total CSA (mm ²)	2.031±0.174	2.068±0.193	2.011±0.216	2.053±0.190
Marrow Area (mm ²)	1.051±0.100	1.047±0.116	1.027±0.104	1.028±0.102
Cortical Area (mm ²)	0.980±0.113	1.020±0.084	0.984±0.129	1.024±0.107
Cortical Th. (mm)	0.227±0.021	0.235±0.010	0.230±0.021	0.238±0.017
Periosteal Pm. (mm)	5.868±0.231	5.921±0.239	5.852±0.271	5.898±0.240
Endocortical Pm. (mm)	4.581±0.224	4.533±0.242	4.530±0.282	4.500±0.218
I _{max} (mm ⁴)	0.346±0.064	0.366±0.061	0.347±0.074	0.366±0.067
I _{min} (mm ⁴)	0.168±0.031	0.177±0.035	0.165±0.041	0.174±0.035
TMD (g/cm ³)	1.272±0.021	1.267±0.048	1.277±0.024	1.280±0.021

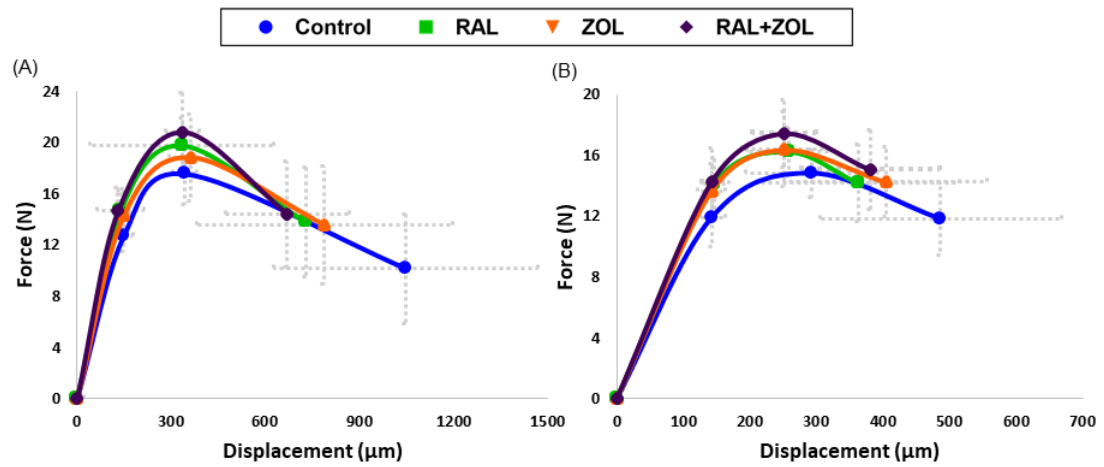
Table 3.2: OIM+/- Cortical Geometry

Property	Control	RAL	ZOL	RAL+ZOL
Total CSA(mm ²)	1.897±0.267	1.837±0.167	1.965±0.310	1.834±0.194
Marrow Area (mm ²)	0.974±0.128	0.902±0.096	0.979±0.157	0.906±0.116
Cortical Area (mm ²)	0.923±0.179	0.935±0.092	0.987±0.176	0.929±0.091
Cortical Th. (mm)	0.225±0.040	0.231±0.017	0.238±0.036	0.229±0.013
Periosteal Pm. (mm)	5.684±0.357	5.630±0.250	5.789±0.395	5.611±0.254
Endocortical Pm. (mm)	4.414±0.301	4.286±0.265	4.513±0.543	4.247±0.256
I _{max} (mm ⁴)	0.300±0.084	0.301±0.058	0.329±0.081	0.292±0.058
I _{min} (mm ⁴)	0.151±0.045	0.139±0.025	0.166±0.073	0.142±0.032
TMD (g/cm ³)	1.309±0.032	1.314±0.031	1.307±0.035	1.314±0.037

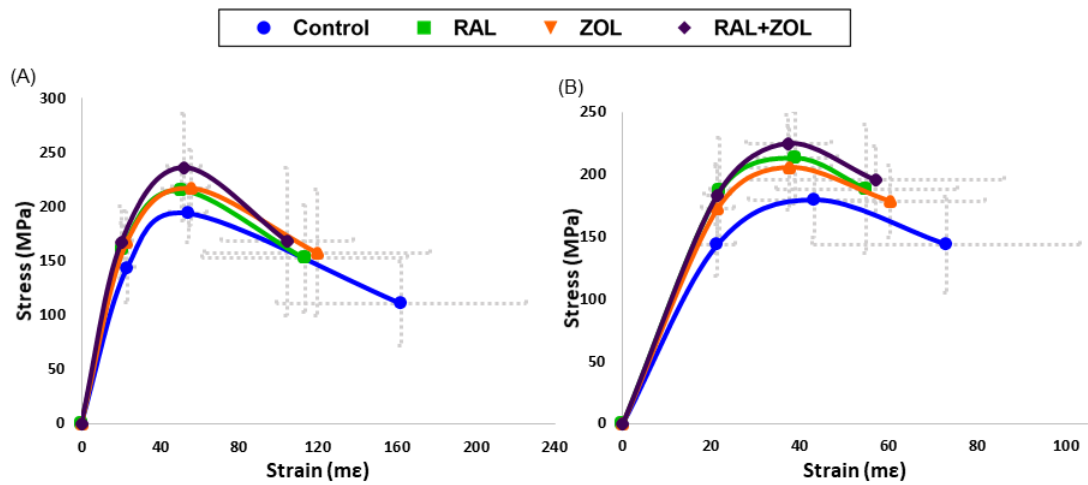
3.3 Femoral Mechanical Strength and Stiffness

The majority of significant effects noted in femoral mechanical properties versus control occurred in strength parameters (Fig. 3.2, Table 3.3-3.6). At the structural level, RAL monotherapy and combination treatment resulted in higher yield force in both genotypes. ZOL monotherapy also significantly increased the property but only in WT. Ultimate force was significantly elevated versus control by the combination treatment in both genotypes. At the tissue level, ultimate stress was significantly higher with combination treatment compared to control in both genotypes. RAL alone increased ultimate stress in OIM+/- but not in WT. Yield stress significantly increased with all treatments in OIM+/- . Although the property trended up in WT, it did not reach significance (ANOVA $p=0.10$). Increased yield stress led to increased resilience in OIM+/- with RAL and combination treatment versus control, but not with ZOL alone.

A few non-strength parameters were also impacted by treatment. Stiffness was significantly higher with all treatments in OIM +/-, but in WT, only increased with RAL monotherapy and combination therapy. The combination treatment in WT also resulted in greater modulus and decreased total strain compared to control.



(a) Schematic Force-Displacement Curves for WT (A) and OIM +/- (B)



(b) Schematic Stress-Strain Curves for WT (A) and OIM +/- (B)

Fig. 3.2: Treatment Effects on Mechanical Properties.

Table 3.3: WT Structural Mechanical Properties

Property	Control	RAL	ZOL	RAL+ZOL
Yield Force (N)	12.7±1.3	14.7±1.6*	14.3±2.0*	14.7±1.8*
Ultimate Force (N)	17.6±2.4	19.8±2.1	18.8±3.4	20.8±3.1*
Displ. to Yield (μm)	148.4±30.6	138.5±21.9	148.8±17.3	130.6±12.8
Postyield Displ. (μm)	899.9±417.0	590.8±291.5	638.9±395.6	539.6±196.0*
Total Displ. (μm)	1048.3±421.5	729.3±292.5*	787.8±407.1	670.2±197.6*
Stiffness (N/mm)	97.7±18.9	120.1±19.7*	107.9±21.7	125.8±14.5*
Work to Yield (mJ)	1.02±0.23	1.11±0.23	1.15±0.17	1.05±0.20
Postyield Work (mJ)	11.20±4.29	9.46±4.33	9.36±4.27	9.62±3.52
Total Work (mJ)	12.22±4.22	10.57±4.37	10.51±4.37	10.67±3.60

Table 3.4: OIM+/- Structural Mechanical Properties

Property	Control	RAL	ZOL	RAL+ZOL
Yield Force (N)	11.9±2.0	14.1±1.7*	13.7±1.8	14.3±2.2*
Ultimate Force (N)	14.8±1.6	16.2±1.6	16.4±2.5	17.4±2.2*
Displ. to Yield (μm)	142.9±18.9	147.0±12.8	142.1±20.4	142.8±16.1
Postyield Displ. (μm)	343.8±177.3	215.7±120.3	261.7±156.5	238.2±100.6
Total Displ. (μm)	486.6±181.4	362.7±121.6	403.9±152.0	381.0±104.3
Stiffness (N/mm)	92.4±9.9	107.0±14.5*	107.9±17.0*	111.5±16.0*
Work to Yield (mJ)	0.93±0.25	1.13±0.19	1.06±0.25	1.12±0.24
Postyield Work (mJ)	4.61±2.49	3.10±1.51	3.97±2.48	3.79±1.69
Total Work (mJ)	5.54±2.55	4.23±1.47	5.03±2.50	4.90±1.82

Table 3.5: WT Tissue-Level Mechanical Properties

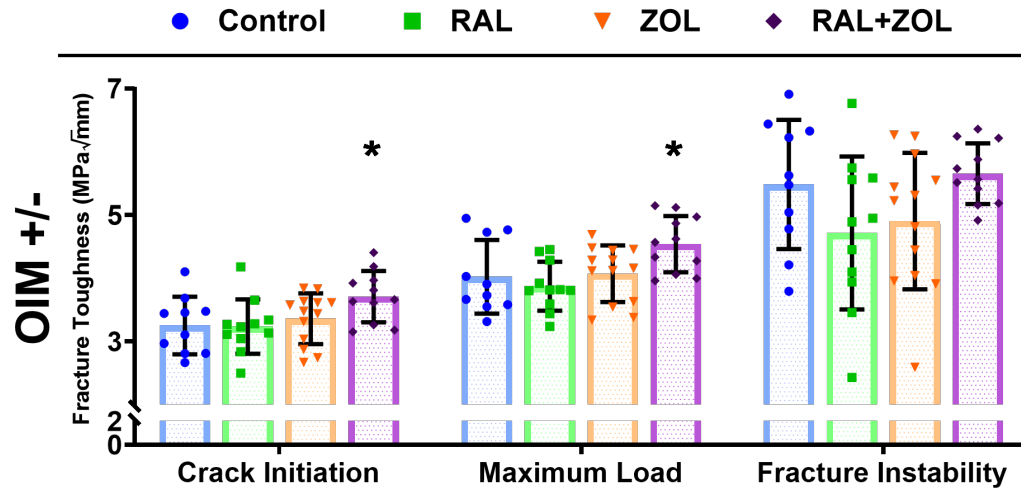
Property	Control	RAL	ZOL	RAL+ZOL
Yield Stress (MPa)	143.0±30.8	161.0±24.3	167.2±29.5	167.3±33.7
Ultimate Stress (MPa)	194.3±26.7	215.5±20.3	217.7±35.5	236.6±49.3*
Strain to Yield ($\mu\epsilon$)	22914±3944	21046±3527	22730±2826	20105±1851
Total Strain ($\mu\epsilon$)	162283±63490	113172±52024	119577±57193	104288±33407*
Modulus (GPa)	6.92±1.19	8.65±1.60	8.33±2.54	9.39±2.34*
Resilience (MPa)	1.80±0.62	1.85±0.49	2.03±0.35	1.83±0.39
Toughness (MPa)	21.30±7.60	17.34±6.27	18.53±7.63	18.28±5.71

Table 3.6: OIM+/- Tissue-Level Mechanical Properties

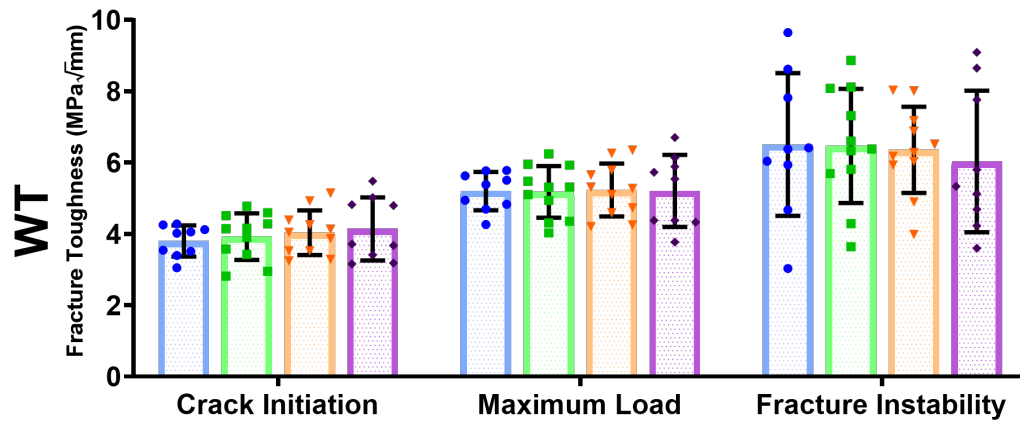
Property	Control	RAL	ZOL	RAL+ZOL
Yield Stress (MPa)	143.3±24.4	187.0±42.5*	172.5±35.6*	183.2±17.4*
Ultimate Stress (MPa)	179.3±30.5	213.3±37.1*	205.4±34.0	224.7±23.3*
Strain to Yield ($\mu\epsilon$)	21270±4099	21929±2287	21418±3764	21303±3255
Total Strain ($\mu\epsilon$)	72862±30109	54960±20533	60239±21398	57002±16760
Modulus (GPa)	7.74±2.19	9.69±3.20	9.09±2.11	9.76±1.82
Resilience (MPa)	1.64±0.38	2.20±0.43*	2.03±0.69	2.13±0.40*
Toughness (MPa)	9.66±4.03	8.12±2.68	9.15±3.8	9.23±2.78

3.4 The Effect of Combination Treatment on Fracture Toughness

Combination treatment in OIM+/- led to significantly higher stress intensity factors at crack initiation and maximum load (Fig. 3.3). Neither monotherapy significantly changed fracture toughness in OIM+/. Treatment in WT produced no significant effects in the stress intensity factors.



(a) Fracture Toughness of OIM+/- at Crack Initiation, Maximum Load, and Failure



(b) Fracture Toughness of WT at Crack Initiation, Maximum Load, and Failure

Fig. 3.3: Effects of Treatment on Fracture Toughness.

CHAPTER 4. CONCLUSION

4.1 Discussion

Current therapeutics used to combat bone fragility are insufficient on their own to optimize bone quality and improve fracture resistance in diseased states. Targeting different mechanisms with a combination treatment could be a potentially powerful technique to enhance bone on both a macroscopic and tissue level. The goal of this study was to investigate how the mass-based effects of bisphosphonates, combined with the tissue-level improvements seen with raloxifene, would improve bone quantity, quality, and fracture resistance. The results demonstrate that ZOL and RAL could be used together to enhance trabecular architecture, cortical mechanical properties, and tissue fracture toughness more than either treatment alone, especially in diseased bone.

For trabecular architecture, the combination treatment appeared to be following the dominant effects of ZOL with an increase in bone volume fraction and trabecular number and a decrease in trabecular spacing. ZOL did not impact trabecular thickness. These trabecular findings are consistent with previous research investigating BPs use in adolescent OI mice. [42–45] The results are unsurprising as at this relatively young age, trabecular bone is often lost with longitudinal growth coupled with resorptive modeling. BP use effectively inhibited this modeling and, thus, maintained bone volume.

Although RAL exhibited an overall minimal effect on trabecular structure, there was a trend toward increased trabecular thickness which contributed to a substantial elevation of thickness when combined with ZOL in both genotypes. RAL alone also led

to increased tissue mineral density. TMD markedly amplified with the combination therapy, potentially since more bone was available to mineralize due to the mass-based effects of ZOL. Male mice were used in this study to limit the cellular metabolic actions of RAL through ER signaling. This suggests that RAL in males may produce quality-based tissue changes through mostly cell-independent mechanism. Similar changes have previously been noted with RAL use. [37, 43]

There were no significant effects on cortical geometry with any treatment in either genotype. In cortical bone, metabolic activity is lower, and it was expected that ZOL would have little effect on mass. [42–45] RAL is also expected to have limited geometric effect in cortical locations, however, previous research has demonstrated significant increases in cortical thickness that were not reproduced in this study. [37, 43] This discrepancy could be due to differences in animal age, background strain, or vendor. Regardless, the lack of geometric changes suggests that any differences in mechanic properties are most likely driven by changes at the intrinsic tissue level.

The significant effects of treatment versus control on mechanical behavior were mostly related to strength parameters. ZOL had a modest impact on its own, significantly increasing yield force in WT and yield stress in OIM+/- . The effects of RAL alone were more compelling, and drove the changes also seen with combination treatment. Yield stress increased in OIM+/- with RAL and combination treatment which led to a significant increase in resilience, indicating the bones were able to absorb more energy before yielding. Unlike previous work with RAL, post yield mechanical behavior was not affected. [34, 37, 43] Here, control groups from both genotypes showed far more total deformation than expected based on previous work with this age and sex of mouse, and the majority of this deformation occurred post yield. It is not clear why this was the case, but it removed the possibility of detecting post yield effects of treatment if they exist. The tissues also stiffened with all the treatments. Bone tissue is known to stiffen with BPs, however, a significant increase in stiffness is somewhat unexpected with RAL. [34, 37, 43] As noted above, these discrepancies could be based on differences in the mice used in this study. Regardless, the net result

is that treatment improved stiffness and strength parameters in bone, and the effect was most pronounced with combination therapy.

Perhaps the most important finding here is that the combination treatment improved stress intensity factors at crack initiation and maximum load in the diseased mice. This type of test reflects true material-level properties in bone and indicates improved fracture resistance in diseased bone with this combined treatment. Treatment did not impact WT mice, likely because it is difficult to improve bone that is already of good quality. Previous work with RAL showed an increase in maximum load toughness with treatment, but RAL alone did not produce the same effects here. This could be due to differences in sample sizes or discrepancies with the notching technique used. Similar to the results of this study, fracture toughness has not been shown to improve with BP treatment. In skeletally mature rabbits, ZOL injections did not improve fracture toughness on ulnar sections. [46] In humans, long term BP use has even been shown to compromise fracture toughness on femoral corticocancellous biopsies. [47]

BPs are the only FDA approved drug for pharmaceutical treatment of Osteogenesis Imperfecta. A recent review paper compiled over 15 years of clinical trials investigating BPs use in patients with OI. It was determined that while both oral and IV BPs substantially improved BMD, it was unclear whether BPs consistently improve fracture resistance and decrease fracture risk. Continuous use of BPs in children and teenagers with OI has revealed some negative impacts on bone health, including microdamage accumulation, delayed healing, and increased mineralization. [48–50] These findings confirm the need for treatments that focus on improving bone quality, in addition to quantity, to improve skeletal fragility and prevent fracture. The fact that we have shown a positive combined treatment effect on measures of fracture resistance in diseased bone, effectively returning these properties to near WT control levels, is promising and future work will focus on treatment strategies to optimize this effect.

4.2 Limitations and Future Work

There are some limitations to our study. Male mice were chosen in attempt to reduce the metabolic effects of RAL and utilize its cell-independent mechanism. This was intentional, but could limit the findings. Future work should be conducted to assess treatment effects on both sexes. With fracture toughness testing, sample sizes were not consistent across groups. Numerous bones were accidentally broken during the notching process. It was also difficult to determine the transition lines of crack propagation for several samples. Homozygous (OIM^{-/-}) mice were originally included in this study. However, the severity of the phenotype caused numerous spontaneous fractures in the untreated mice, and only 2 control samples were usable for analysis. Lastly, the age of the mice used here could be controversial. The mice received treatment from 8 weeks to 16 weeks. The age group was chosen to mirror the rapid growth during human adolescence, and potentially when treatment might be started in humans with OI. This age could have led to the high deformation in the control groups due to rapid modeling and slow mineralization. It is also problematic because it does not coincide with an age that humans receive RAL, as RAL is typically only administered in older adults. Future studies will also investigate the effects of combined treatment in older animals, following skeletal maturity.

The use of RAL has some limitations in itself. Although RAL possesses beneficial intrinsic effects, it may not necessarily be the most ideal drug to pursue for combinatorial therapy. RAL suppresses bone loss as a selective estrogen receptor modulator (SERM), but this estrogen therapy produces adverse effects such as hot flashes and increased thrombosis risk, making it a problematic treatment. The estrogen receptor binding also prevents usage in some at-risk patient populations including children, specifically those with OI. [51, 52] Other drugs could be considered for a combination treatment. Recent work has shown positive outcomes in OI patients and OI mice treated with sclerostin antibody and denosumab. [45, 53, 54] These compounds,

amongst others, should be investigated to determine an ideal combination and dosing schedule.

In conclusion, the current study shows beneficial effects of combination therapy to enhance quality of diseased bone in a way that neither treatment could accomplish alone. Utilizing the mass-based effects of ZOL with the tissue material changes of RAL, the combination therapy improved fracture toughness in addition to increases in trabecular architecture and cortical mechanics, especially in diseased animals. Combinatorial treatments should be considered for future therapies to optimize patient care and bone health.

LIST OF REFERENCES

LIST OF REFERENCES

- [1] D. B. Burr and O. Akkus, *Chapter 1 - Bone Morphology and Organization*. San Diego: Academic Press, 2014, pp. 3–25.
- [2] M. C. van der Meulen, K. J. Jepsen, and B. Mikic, “Understanding bone strength: size isn’t everything,” *Bone*, vol. 29, no. 2, pp. 101–4, 2001.
- [3] E. Donnelly, “Methods for assessing bone quality: a review,” *Clin Orthop Relat Res*, vol. 469, no. 8, pp. 2128–38, 2011.
- [4] S. Judex, S. Boyd, Y. X. Qin, L. Miller, R. Muller, and C. Rubin, “Combining high-resolution micro-computed tomography with material composition to define the quality of bone tissue,” *Curr Osteoporos Rep*, vol. 1, no. 1, pp. 11–9, 2003.
- [5] E. Seeman and P. D. Delmas, “Bone quality—the material and structural basis of bone strength and fragility,” *N Engl J Med*, vol. 354, no. 21, pp. 2250–61, 2006.
- [6] M. E. Launey, M. J. Buehler, and R. O. Ritchie, “On the mechanistic origins of toughness in bone,” *Annual Review of Materials Research*, vol. 40, no. 1, pp. 25–53, 2010.
- [7] G. O. of the Surgeon, *Reports of the Surgeon General*. Rockville (MD): Office of the Surgeon General (US), 2004.
- [8] M. Saito and K. Marumo, “Collagen cross-links as a determinant of bone quality: a possible explanation for bone fragility in aging, osteoporosis, and diabetes mellitus,” *Osteoporos Int*, vol. 21, no. 2, pp. 195–214, 2010.
- [9] E. A. Imel, L. A. DiMeglio, and D. B. Burr, *Chapter 16 - Metabolic Bone Diseases*. San Diego: Academic Press, 2014, pp. 317–344.
- [10] J. C. Marini, A. Forlino, W. A. Cabral, A. M. Barnes, J. D. San Antonio, S. Milgrom, J. C. Hyland, J. Korkko, D. J. Prockop, A. De Paepe, P. Coucke, S. Symoens, F. H. Glorieux, P. J. Roughley, A. M. Lund, K. Kuurila-Svahn, H. Hartikka, D. H. Cohn, D. Krakow, M. Mottes, U. Schwarze, D. Chen, K. Yang, C. Kuslich, J. Troendle, R. Dalglish, and P. H. Byers, “Consortium for osteogenesis imperfecta mutations in the helical domain of type i collagen: regions rich in lethal mutations align with collagen binding sites for integrins and proteoglycans,” *Hum Mutat*, vol. 28, no. 3, pp. 209–21, 2007.
- [11] D. W. Rowe and J. R. Shapiro, *Osteogenesis Imperfecta*, 3rd ed. Academic Press, 1998, book section 23, pp. 651–683.

- [12] H. Kuivaniemi, G. Tromp, and D. J. Prockop, "Mutations in fibrillar collagens (types i, ii, iii, and xi), fibril-associated collagen (type ix), and network-forming collagen (type x) cause a spectrum of diseases of bone, cartilage, and blood vessels," *Hum Mutat*, vol. 9, no. 4, pp. 300–15, 1997.
- [13] T. Pihlajaniemi, L. A. Dickson, F. M. Pope, V. R. Korhonen, A. Nicholls, D. J. Prockop, and J. C. Myers, "Osteogenesis imperfecta: cloning of a pro-alpha 2(i) collagen gene with a frameshift mutation," *J Biol Chem*, vol. 259, no. 21, pp. 12941–4, 1984.
- [14] T. J. Martin and E. Seeman, "Bone remodelling: its local regulation and the emergence of bone fragility," *Best Pract Res Clin Endocrinol Metab*, vol. 22, no. 5, pp. 701–22, 2008.
- [15] M. R. Allen and D. B. Burr, *Chapter 4 - Bone Modeling and Remodeling*. San Diego: Academic Press, 2014, pp. 75–90.
- [16] T. Bellido, L. I. Plotkin, and A. Bruzzaniti, *Chapter 2 - Bone Cells*. San Diego: Academic Press, 2014, pp. 27–45.
- [17] M. A. Parfitt, *Skeletal Heterogeneity and the Purposes of Bone Remodeling: Implications for the Understanding of Osteoporosis*, 4th ed. Academic Press, 2013, pp. 855–872.
- [18] B. H. Mitlak, D. B. Burr, and M. R. Allen, *Chapter 17 - Pharmaceutical Treatments of Osteoporosis*. San Diego: Academic Press, 2014, pp. 345–363.
- [19] R. G. Russell, "Bisphosphonates: the first 40 years," *Bone*, vol. 49, no. 1, pp. 2–19, 2011.
- [20] NIH, "Osteoporosis prevention, diagnosis, and therapy," *JAMA*, vol. 285, no. 6, pp. 785–95, 2001.
- [21] F. H. Glorieux, N. J. Bishop, H. Plotkin, G. Chabot, G. Lanoue, and R. Travers, "Cyclic administration of pamidronate in children with severe osteogenesis imperfecta," *N Engl J Med*, vol. 339, no. 14, pp. 947–52, 1998.
- [22] R. G. Russell, N. B. Watts, F. H. Ebetino, and M. J. Rogers, "Mechanisms of action of bisphosphonates: similarities and differences and their potential influence on clinical efficacy," *Osteoporos Int*, vol. 19, no. 6, pp. 733–59, 2008.
- [23] M. R. Allen and D. B. Burr, "Bisphosphonate effects on bone turnover, microdamage, and mechanical properties: what we think we know and what we know that we don't know," *Bone*, vol. 49, no. 1, pp. 56–65, 2011.
- [24] M. R. Allen, E. Gineyts, D. J. Leeming, D. B. Burr, and P. D. Delmas, "Bisphosphonates alter trabecular bone collagen cross-linking and isomerization in beagle dog vertebra," *Osteoporos Int*, vol. 19, no. 3, pp. 329–37, 2008.
- [25] S. Y. Tang, M. R. Allen, R. Phipps, D. B. Burr, and D. Vashishth, "Changes in non-enzymatic glycation and its association with altered mechanical properties following 1-year treatment with risedronate or alendronate," *Osteoporos Int*, vol. 20, no. 6, pp. 887–94, 2009.

- [26] C. Acevedo, H. Bale, B. Gludovatz, A. Wat, S. Y. Tang, M. Wang, B. Busse, E. A. Zimmermann, E. Schaible, M. R. Allen, D. B. Burr, and R. O. Ritchie, "Alendronate treatment alters bone tissues at multiple structural levels in healthy canine cortical bone," *Bone*, vol. 81, pp. 352–363, 2015.
- [27] H. U. Bryant, "Mechanism of action and preclinical profile of raloxifene, a selective estrogen receptor modulation," *Rev Endocr Metab Disord*, vol. 2, no. 1, pp. 129–38, 2001.
- [28] B. Ettinger, D. M. Black, B. H. Mitlak, R. K. Knickerbocker, T. Nickelsen, H. K. Genant, C. Christiansen, P. D. Delmas, J. R. Zanchetta, J. Stakkestad, C. C. Gluer, K. Krueger, F. J. Cohen, S. Eckert, K. E. Ensrud, L. V. Avioli, P. Lips, and S. R. Cummings, "Reduction of vertebral fracture risk in postmenopausal women with osteoporosis treated with raloxifene: results from a 3-year randomized clinical trial. multiple outcomes of raloxifene evaluation (more) investigators," *JAMA*, vol. 282, no. 7, pp. 637–45, 1999.
- [29] R. R. Recker, B. H. Mitlak, X. Ni, and J. H. Krege, "Long-term raloxifene for postmenopausal osteoporosis," *Curr Med Res Opin*, vol. 27, no. 9, pp. 1755–61, 2011.
- [30] E. Seeman, G. G. Crans, A. Diez-Perez, K. V. Pinette, and P. D. Delmas, "Anti-vertebral fracture efficacy of raloxifene: a meta-analysis," *Osteoporos Int*, vol. 17, no. 2, pp. 313–6, 2006.
- [31] M. A. Gallant, D. M. Brown, M. Hammond, J. M. Wallace, J. Du, A. C. Deymier-Black, J. D. Almer, S. R. Stock, M. R. Allen, and D. B. Burr, "Bone cell-independent benefits of raloxifene on the skeleton: a novel mechanism for improving bone material properties," *Bone*, vol. 61, pp. 191–200, 2014.
- [32] N. Bivi, H. Hu, B. Chavali, M. J. Chalmers, C. T. Reutter, G. L. Durst, A. Riley, M. Sato, M. R. Allen, D. B. Burr, and J. A. Dodge, "Structural features underlying raloxifene's biophysical interaction with bone matrix," *Bioorg Med Chem*, vol. 24, no. 4, pp. 759–67, 2016.
- [33] A. Carriero, E. A. Zimmermann, A. Paluszny, S. Y. Tang, H. Bale, B. Busse, T. Alliston, G. Kazakia, R. O. Ritchie, and S. J. Shefelbine, "How tough is brittle bone? investigating osteogenesis imperfecta in mouse bone," *J Bone Miner Res*, vol. 29, no. 6, pp. 1392–1401, 2014.
- [34] M. R. Allen, H. A. Hogan, W. A. Hobbs, A. S. Koivuniemi, M. C. Koivuniemi, and D. B. Burr, "Raloxifene enhances material-level mechanical properties of femoral cortical and trabecular bone," *Endocrinology*, vol. 148, no. 8, pp. 3908–13, 2007.
- [35] M. R. Allen, P. R. Territo, C. Lin, S. Persohn, L. Jiang, A. A. Riley, B. P. McCarthy, C. L. Newman, D. B. Burr, and G. D. Hutchins, "In vivo uterine MRI reveals positive effects of raloxifene on skeletal-bound water in skeletally mature beagle dogs," *J Bone Miner Res*, vol. 30, no. 8, pp. 1441–4, 2015.
- [36] M. W. Aref, E. M. McNerny, D. Brown, K. J. Jepsen, and M. R. Allen, "Zoledronate treatment has different effects in mouse strains with contrasting baseline bone mechanical phenotypes," *Osteoporos Int*, vol. 27, no. 12, pp. 3637–3643, 2016.

- [37] A. G. Berman, J. M. Wallace, Z. R. Bart, and M. R. Allen, "Raloxifene reduces skeletal fractures in an animal model of osteogenesis imperfecta," *Matrix Biol*, vol. 52-54, pp. 19–28, 2016.
- [38] A. G. Berman, C. A. Clauser, C. Wunderlin, M. A. Hammond, and J. M. Wallace, "Structural and mechanical improvements to bone are strain dependent with axial compression of the tibia in female c57bl/6 mice," *PLoS One*, vol. 10, no. 6, p. e0130504, 2015.
- [39] J. M. Wallace, K. Golcuk, M. D. Morris, and D. H. Kohn, "Inbred strain-specific response to biglycan deficiency in the cortical bone of c57bl/129 and c3h/he mice," *J Bone Miner Res*, vol. 24, no. 6, pp. 1002–12, 2009.
- [40] R. O. Ritchie, K. J. Koester, S. Ionova, W. Yao, N. E. Lane, and r. Ager, J. W., "Measurement of the toughness of bone: a tutorial with special reference to small animal studies," *Bone*, vol. 43, no. 5, pp. 798–812, 2008.
- [41] M. A. Hammond, A. G. Berman, R. Pacheco-Costa, H. M. Davis, L. I. Plotkin, and J. M. Wallace, "Removing or truncating connexin 43 in murine osteocytes alters cortical geometry, nanoscale morphology, and tissue mechanics in the tibia," *Bone*, vol. 88, pp. 85–91, 2016.
- [42] R. Bargman, R. Posham, A. L. Boskey, E. DiCarlo, C. Raggio, and N. Pleshko, "Comparable outcomes in fracture reduction and bone properties with rankl inhibition and alendronate treatment in a mouse model of osteogenesis imperfecta," *Osteoporos Int*, vol. 23, no. 3, pp. 1141–50, 2012.
- [43] C. N. Meixner, M. W. Aref, A. Gupta, E. M. B. McNerny, D. Brown, J. M. Wallace, and M. R. Allen, "Raloxifene improves bone mechanical properties in mice previously treated with zoledronate," *Calcif Tissue Int*, vol. 101, no. 1, pp. 75–81, 2017.
- [44] B. M. Misof, P. Roschger, T. Baldini, C. L. Raggio, V. Zraick, L. Root, A. L. Boskey, K. Klaushofer, P. Fratzl, and N. P. Camacho, "Differential effects of alendronate treatment on bone from growing osteogenesis imperfecta and wild-type mouse," *Bone*, vol. 36, no. 1, pp. 150–8, 2005.
- [45] D. Olvera, R. Stolzenfeld, J. C. Marini, M. S. Caird, and K. M. Kozloff, "Low dose of bisphosphonate enhances sclerostin antibody-induced trabecular bone mass gains in brtl/+ osteogenesis imperfecta mouse model," *J Bone Miner Res*, vol. 33, no. 7, pp. 1272–1282, 2018.
- [46] M. D. Hunckler, E. D. Chu, A. P. Baumann, T. E. Curtis, M. J. Ravosa, M. R. Allen, and R. K. Roeder, "The fracture toughness of small animal cortical bone measured using arc-shaped tension specimens: Effects of bisphosphonate and deproteinization treatments," *Bone*, vol. 105, pp. 67–74, 2017.
- [47] A. A. Lloyd, B. Gludovatz, C. Riedel, E. A. Luengo, R. Saiyed, E. Marty, D. G. Lorch, J. M. Lane, R. O. Ritchie, B. Busse, and E. Donnelly, "Atypical fracture with long-term bisphosphonate therapy is associated with altered cortical composition and reduced fracture resistance," *Proc Natl Acad Sci U S A*, vol. 114, no. 33, pp. 8722–8727, 2017.

- [48] E. A. Anam, F. Rauch, F. H. Glorieux, F. Fassier, and R. Hamdy, "Osteotomy healing in children with osteogenesis imperfecta receiving bisphosphonate treatment," *J Bone Miner Res*, vol. 30, no. 8, pp. 1362–8, 2015.
- [49] S. E. Papapoulos and S. C. Cremers, "Prolonged bisphosphonate release after treatment in children," *N Engl J Med*, vol. 356, no. 10, pp. 1075–6, 2007.
- [50] R. F. Vasanwala, A. Sanghrajka, N. J. Bishop, and W. Hogler, "Recurrent proximal femur fractures in a teenager with osteogenesis imperfecta on continuous bisphosphonate therapy: Are we overtreating?" *J Bone Miner Res*, vol. 31, no. 7, pp. 1449–54, 2016.
- [51] A. Qaseem, M. A. Forciea, R. M. McLean, and T. D. Denberg, "Treatment of low bone density or osteoporosis to prevent fractures in men and women: A clinical practice guideline update from the american college of physicians," *Ann Intern Med*, vol. 166, no. 11, pp. 818–839, 2017.
- [52] I. R. Reid, "Efficacy, effectiveness and side effects of medications used to prevent fractures," *J Intern Med*, vol. 277, no. 6, pp. 690–706, 2015.
- [53] F. H. Glorieux, J. P. Devogelaer, M. Durigova, S. Goemaere, S. Hemsley, F. Jakob, U. Junker, J. Ruckle, L. Seefried, and P. J. Winkle, "Bps804 anti-sclerostin antibody in adults with moderate osteogenesis imperfecta: Results of a randomized phase 2a trial," *J Bone Miner Res*, vol. 32, no. 7, pp. 1496–1504, 2017.
- [54] H. Hoyer-Kuhn, J. Franklin, G. Allo, M. Kron, C. Netzer, P. Eysel, B. Hero, E. Schoenau, and O. Semler, "Safety and efficacy of denosumab in children with osteogenesis imperfect—a first prospective trial," *J Musculoskelet Neuronal Interact*, vol. 16, no. 1, pp. 24–32, 2016.